

## Josephson phase qubit with an optimal point

Norihito Kosugi,<sup>1</sup> Shigemasa Matsuo,<sup>1,2</sup> Toshiyuki Fujii,<sup>1</sup> and Noriyuki Hatakenaka<sup>1</sup>

<sup>1</sup>*Graduate School of Integrated Arts and Sciences, Hiroshima University, Higashi-Hiroshima 739-8521, Japan*

<sup>2</sup>*Research Institute for Science and Engineering, Waseda University, Shinjuku-ku, Tokyo 169-8555, Japan*

(Received 8 September 2009; revised manuscript received 22 November 2009; published 11 January 2010)

Current fluctuations in a Josephson phase qubit are considered to be a source of decoherence, especially for pure dephasing. One possible way of evading such decoherence is to employ an optimal operation point as used in flux and charge qubits, where the qubit is insensitive to the bias fluctuations. However, there is no optimal point in a phase qubit since qubit energy splitting becomes monotonically smaller with increasing the bias current. Here we propose a phase qubit with an optimal point by introducing qubit energy splitting that depends *nonmonotonically* on the current bias realized in capacitively coupled Josephson junctions. The effect of junction asymmetry on the optimal point is also investigated.

DOI: 10.1103/PhysRevB.81.024507

PACS number(s): 03.65.Yz, 03.67.-a, 03.75.Lm, 42.88.+h

### I. INTRODUCTION

A superconducting qubit that is based on a superconducting circuit incorporating small Josephson junctions is a promising candidate for a qubit as a building block for quantum computer owing to its scalability. There are basically three types of superconducting qubits, namely, flux,<sup>1,2</sup> charge,<sup>3,4</sup> and phase<sup>5-7</sup> qubits which can be operated by controlling the flux, the gate voltage, and the current biases, respectively. Unfortunately, the decoherence times of such superconducting qubits, which should be much longer than the manipulation times, are insufficient for scalable quantum computation and error correction with current techniques.

Two types of decoherence processes in superconducting qubits have been considered.<sup>8</sup> (i) Energy relaxation is a process which the excited state of a two-level system returns to the ground state by transferring energy to the environment. The energy relaxation inevitably occurs in a nonequilibrium system which reverts to an equilibrium system.<sup>9</sup> (ii) Pure dephasing is the decay of coherence without a change in the two-level populations. Pure dephasing is usually caused by inhomogeneous level broadening in ensembles of two-level systems but also occurs even in a single two-level system due to the low-frequency fluctuation of the energy separation induced by the fluctuations of biases.<sup>10</sup> The suppression of these decoherence processes is a key issue as regards implementing quantum computers.

Energy relaxation can be controlled in a superconducting qubit with a carefully designed environment modeled by a single-mode/multimode cavity.<sup>11</sup> While, pure dephasing can be greatly suppressed with a special bias operating the qubit, called an optimal point, where the qubit is insensitive to fluctuations induced by the external biases. In fact, flux<sup>12</sup> and charge<sup>13</sup> qubits become insensitive to flux and charge fluctuations, respectively, at the optimal point as a result of the symmetric features of energy separation in relation to operation biases. In this case, decoherence is mainly induced by the energy relaxation. However, there is no optimal point in a phase qubit. Recently, Hoskinson *et al.*<sup>14</sup> reported an optimal point in a dc-superconducting quantum interference device (SQUID)-based phase qubit. Indeed, their phase qubit became insensitive to the fluctuation of total current through

the dc-SQUID acting as a phase qubit. However, an alternative noise appears due to the loop structure of the dc-SQUID, i.e., flux fluctuation. Unfortunately, there is no optimal point for this fluctuation. Therefore, there are still no actual optimal points in phase qubits.

In this paper, we propose to equip a phase qubit with an optimal point by introducing a symmetric feature of qubit energy splitting with regard to current bias in coupled current-biased Josephson junctions (CBJJs). In Sec. II, we investigate the dynamics of the coupled CBJJs interacting with the environment by using the equation of motion for a reduced density matrix within the Born-Markov approximation (Bloch-Redfield equation),<sup>15,16</sup> in order to obtain an analytic expression for pure dephasing. In Sec. III, we investigate an optimal point in the coupled Josephson-phase qubit based on the pure dephasing formula. The last section provides the conclusion to this paper.

### II. BLOCH-REDFIELD THEORY OF PHASE QUBITS BASED ON CAPACITIVELY COUPLED JOSEPHSON JUNCTIONS

#### A. System and Hamiltonian

The system we consider is phase qubits based on capacitively coupled CBJJs interacting with the environment as shown in Fig. 1. The total Hamiltonian is written as<sup>17</sup>

$$\hat{H}^{tot} = \hat{H}^{sys} + \hat{H}^{env} + \hat{H}^{int}. \quad (1)$$

The first term in Eq. (1) describes a system Hamiltonian consisting of two Josephson junctions and their coupling, written as (refer to Appendix)<sup>18,19</sup>

$$\hat{H}^{sys} = \sum_{i=A,B} \hat{H}_i^{sys} + \hat{H}_{AB}^{sys}, \quad (2)$$

$$\hat{H}_i^{sys} = \frac{\hat{p}_i^2}{2\tilde{C}_i} + \hat{U}_i, \quad (3)$$

$$\hat{U}_i = E_{Ji}(1 - \cos \hat{\theta}_i - \tilde{I}_i \hat{\theta}_i), \quad (4)$$

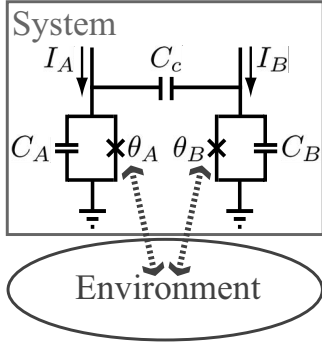


FIG. 1. Circuit diagram for a system consisting of two capacitively coupled CBJJs interacting with the environment.  $I_i$  and  $\theta_i$  are the current bias and the phase difference across the  $i$ th junction ( $i=A$  or  $B$ ), respectively.  $C_i$  and  $C_c$  are the capacitance of the  $i$ th junction and the capacitance between two junctions, respectively.

$$\hat{H}_{AB}^{sys} = \sqrt{\delta_A \delta_B} \frac{\hat{P}_A \hat{P}_B}{\sqrt{\tilde{C}_A \tilde{C}_B}}. \quad (5)$$

The  $i$ th junction has a critical current  $I_{ci}$ , a junction capacitance  $C_i$ , a Josephson energy  $E_{Ji}$ , and a phase difference across the junction  $\theta_i$  under the current bias  $I_i$  ( $i=A$  or  $B$ ). The effective capacitance  $\tilde{C}_i$  is given by  $C_i + (C_j^{-1} + C_c^{-1})^{-1}$  with  $C_c$  being the coupling capacitance ( $i \neq j$ ). The momentum operator  $\hat{p}_i$  is given by  $-i\hbar(2\pi/\Phi_0)\partial/\partial\theta_i$  with  $\hat{\theta}_i$  being the phase operator. The coupling parameter  $\delta_i$  and the normalized current  $\tilde{I}_i$  are given by  $C_c/(C_i + C_c)$  and  $I_i/I_{ci}$ , res-

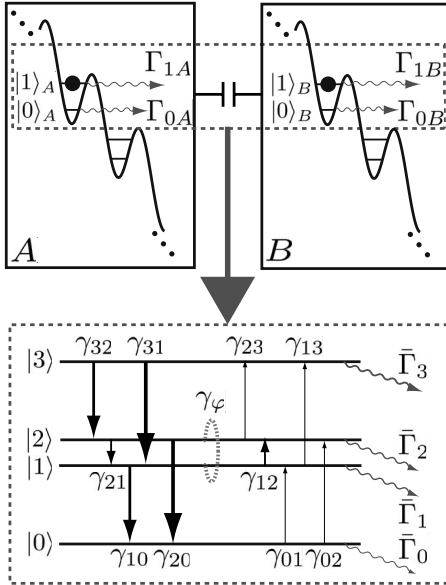


FIG. 2. Energy-level diagram for coupled junctions in the presence of dissipation. Here  $\gamma_{ij}$  indicates the energy-relaxation rate related to the relaxation from the  $i$ th level to the  $j$ th level, where  $i$  and  $j$  are integers running from 0–3.  $\Gamma_{kA}$  ( $\Gamma_{kB}$ ) denotes the tunneling rate from the state  $|k\rangle$  in the Josephson junction  $A$  ( $B$ );  $k$  is the integer 0 or 1. The decay rate from each level  $\bar{\Gamma}_i$  associated with the tunneling rates  $\Gamma_{kA,B}$ .  $\gamma_\varphi$  is the pure dephasing rate.

spectively. In a small-area junction, the energy, a tilted cosine potential (washboard potential), is quantized, and the energy is then represented as a Wannier-Stark ladder.<sup>20</sup> The  $n$ th energy state of the  $i$ th junction  $|n\rangle_i$  has the complex energy  $\mathcal{E}_{ni} - i\hbar\Gamma_{ni}/2$  due to quantum tunneling,<sup>21</sup> where  $\mathcal{E}_{ni}$  denotes the quantized energy of the state  $|n\rangle_i$  and  $\Gamma_{ni}$  is the tunneling rate from the state  $|n\rangle_i$ . Here we assume that only two energy levels are formed in a quantum well in the washboard potential  $U_i$ . These serve as a conventional phase qubit as shown in the upper part of Fig. 2. Hamiltonian  $\hat{H}_i^{sys}$  is then written as

$$\hat{H}_i^{sys} = -\left(\varepsilon_i - i\hbar\frac{\Gamma_{1i} - \Gamma_{0i}}{4}\right)\hat{\sigma}_{zi} - i\hbar\frac{\Gamma_{1i} + \Gamma_{0i}}{4}\hat{1}, \quad (6)$$

where  $\varepsilon_i$  is defined as  $(\mathcal{E}_{1i} - \mathcal{E}_{0i})/2$ . Pauli matrices  $\hat{\sigma}_{ji}$  ( $j=x, y, z$ ) and unit matrix  $\hat{1}$  act in the basis of the states  $|0\rangle_i$  and  $|1\rangle_i$ . The interaction Hamiltonian  $\hat{H}_{AB}^{sys}$  is also written as

$$\begin{aligned} \hat{H}_{AB}^{sys} &= \sqrt{\frac{\delta_A \delta_B}{\tilde{C}_A \tilde{C}_B}} \sum_{k, \ell, n, r=0,1} (|k\rangle\langle k|_A) \hat{p}_A (|\ell\rangle\langle \ell|_A) (|r\rangle\langle r|_B) \hat{p}_B (|n\rangle \\ &\times \langle n|_B), \\ &= \sqrt{\frac{\delta_A \delta_B}{\tilde{C}_A \tilde{C}_B}} \sum_{k, \ell, n, r=0,1} \langle k|\hat{p}_A|\ell\rangle_A \langle r|\hat{p}_B|n\rangle_B \times |k\rangle\langle \ell|_A \otimes |r\rangle \\ &\times \langle n|_B. \end{aligned} \quad (7)$$

The phase qubit is realized at the current bias where the Josephson potential is well approximated by a quadratic-plus-cubic potential. In this case, the quadratic nature of the potential becomes appreciable. Thus, the diagonal matrix elements are ignored ( $|\langle k|\hat{p}_i|k\rangle|_i \ll |\langle k|\hat{p}_i|j\rangle|_i$ ,  $k \neq j$ ). Then, Eq. (7) is rewritten as

$$\begin{aligned} \hat{H}_{AB}^{sys} &\approx g_+ (|0\rangle\langle 1|_A \otimes |0\rangle\langle 1|_B + |1\rangle\langle 0|_A \otimes |1\rangle\langle 0|_B) \\ &+ g_- (|0\rangle\langle 1|_A \otimes |1\rangle\langle 0|_B + |1\rangle\langle 0|_A \otimes |0\rangle\langle 1|_B), \\ &= g_+ (\hat{\sigma}_{+A} \hat{\sigma}_{+B} + \hat{\sigma}_{-A} \hat{\sigma}_{-B}) + g_- (\hat{\sigma}_{+A} \hat{\sigma}_{-B} + \hat{\sigma}_{-A} \hat{\sigma}_{+B}), \end{aligned} \quad (8)$$

where coupling constants  $g_+$  and  $g_-$  are given by

$$g_+ = \sqrt{\delta_A \delta_B / \tilde{C}_A \tilde{C}_B} \langle 0|\hat{p}_A|1\rangle_A \langle 0|\hat{p}_B|1\rangle_B$$

and

$$g_- = \sqrt{\delta_A \delta_B / \tilde{C}_A \tilde{C}_B} \langle 0|\hat{p}_A|1\rangle_A \langle 1|\hat{p}_B|0\rangle_B.$$

Matrices  $\hat{\sigma}_{\pm i}$  are defined as  $\hat{\sigma}_{xi} \pm i\hat{\sigma}_{yi}$ . Eigenstates and eigenenergies with respect to the real part of Eqs. (6) and (8) are given by<sup>22</sup>

$$|0\rangle \equiv \cos\frac{\eta_+}{2}|00\rangle - \sin\frac{\eta_+}{2}|11\rangle, \quad (9)$$

$$|1\rangle \equiv \cos\frac{\eta_-}{2}|01\rangle - \sin\frac{\eta_-}{2}|10\rangle, \quad (10)$$

$$|2\rangle \equiv \sin \frac{\eta_-}{2} |01\rangle + \cos \frac{\eta_-}{2} |10\rangle, \quad (11)$$

$$|3\rangle \equiv \sin \frac{\eta_+}{2} |00\rangle + \cos \frac{\eta_+}{2} |11\rangle, \quad (12)$$

$$E_0 = -\sqrt{(\varepsilon_A + \varepsilon_B)^2 + g_+^2}, \quad (13)$$

$$E_1 = -\sqrt{(\varepsilon_A - \varepsilon_B)^2 + g_-^2}, \quad (14)$$

$$E_2 = \sqrt{(\varepsilon_A - \varepsilon_B)^2 + g_-^2}, \quad (15)$$

$$E_3 = \sqrt{(\varepsilon_A + \varepsilon_B)^2 + g_+^2}, \quad (16)$$

where  $\eta_{\pm}$  is given by  $\tan^{-1}\{g_{\pm}/(\varepsilon_A \pm \varepsilon_B)\}$ . These energy levels are shown in the lower part of Fig. 2. We employ the states  $|1\rangle$  and  $|2\rangle$  as a phase qubit in coupled CBJJs in this paper. As shown in the next section, pure dephasing is greatly suppressed at an optimal operating point.

The second term in Eq. (1) is the Hamiltonian for the environment, which is assumed to be a set of harmonic oscillators written as<sup>23</sup>

$$\hat{H}^{env} = \sum_{\alpha} \hbar \omega_{\alpha} \left( \hat{a}_{\alpha}^{\dagger} \hat{a}_{\alpha} + \frac{1}{2} \right), \quad (17)$$

where  $\omega_{\alpha}$  denotes the frequency of a harmonic oscillator at mode  $\alpha$  in the environment. The operator  $\hat{a}_{\alpha}$  ( $\hat{a}_{\alpha}^{\dagger}$ ) is an annihilation (creation) operator with respect to a harmonic oscillator.

The third term in Eq. (1) is the interaction Hamiltonian between each phase particle and the environment written as

$$\hat{H}^{int} = \hat{\chi} \sum_{\alpha} \lambda_{\alpha} (\hat{a}_{\alpha}^{\dagger} + \hat{a}_{\alpha}), \quad (18)$$

where

$$\hat{\chi} = \sum_{i=A,B} (\zeta_i \hat{\sigma}_{xi} - \xi_i \hat{\sigma}_{zi}) \quad (19)$$

with

$$\zeta_i = \langle 0 | \hat{\theta}_i | 1 \rangle_i, \quad (20)$$

$$\xi_i = \frac{1}{2} (\langle 1 | \hat{\theta}_i | 1 \rangle_i - \langle 0 | \hat{\theta}_i | 0 \rangle_i). \quad (21)$$

Here  $\lambda_{\alpha}$  is a coupling constant between the phase particles and the environment. The coupling interaction has been assumed to be linear in the environment coordinates.<sup>23</sup>

### B. Bloch-Redfield equations

The Bloch-Redfield equations are given from the equations of motion for reduced density-matrix  $\hat{\rho}$  in the basis  $\{|0\rangle, |1\rangle, |2\rangle, |3\rangle\}$  within the Born-Markov approximation as<sup>16</sup>

$$\begin{aligned} \dot{\rho}_{nm} &= -\frac{i}{\hbar} [\hat{H}^{sys} \hat{\rho}(t) - \hat{\rho}(t) (\hat{H}^{sys})^{\dagger}]_{nm} - \sum_{k,\ell} R_{nmk\ell} \rho_{k\ell}, \\ &= -\frac{i}{\hbar} [\text{Re } \hat{H}^{sys}, \hat{\rho}(t)]_{nm} + \frac{1}{\hbar} \{\text{Im } \hat{H}^{sys}, \hat{\rho}(t)\}_{nm} - \sum_{k,\ell} R_{nmk\ell} \rho_{k\ell}, \\ &= -i \omega_{nm} \rho_{nm} + \frac{1}{\hbar} \{\text{Im } \hat{H}^{sys}, \hat{\rho}(t)\}_{nm} - \sum_{k,\ell} R_{nmk\ell} \rho_{k\ell}, \\ &= -i \omega_{nm} \rho_{nm} - \sum_{k,\ell} (T_{nmk\ell} + R_{nmk\ell}) \rho_{k\ell}, \end{aligned} \quad (22)$$

where  $\rho_{nm} = \langle n | \hat{\rho} | m \rangle$  and  $\omega_{nm} = (E_n - E_m) / \hbar$ . The reduced density matrix is obtained by tracing out the density matrix of the environment from the density matrix of the total system. The first term denotes the dynamical motion of the system in terms of the transition frequencies  $\omega_{nm}$ . Here the tensor  $T_{nmk\ell}$  originates from the imaginary part of the system Hamiltonian  $\text{Im } \hat{H}^{sys}$  associated with the process of tunneling from the metastable states  $|0\rangle_{A,B}$  and  $|1\rangle_{A,B}$ .<sup>24,25</sup> The tensor  $R_{nmk\ell}$  connecting  $\rho_{nm}$  to  $\rho_{kl}$  is given by

$$R_{nmk\ell} = \sum_r (\delta_{\ell,m} \Xi_{nrk}^{(+)} + \delta_{n,k} \Xi_{mrr}^{(+*)}) - \Xi_{\ell mnk}^{(+)} - \Xi_{knm\ell}^{(+*)} \quad (23)$$

with

$$\Xi_{\ell mnk}^{(+)} = \frac{1}{\hbar^2} \int_0^{\infty} d\tau e^{-i\omega_{nk}\tau} \times \text{Tr}_{env} [\bar{H}_{\ell m}^{int}(\tau) \bar{H}_{nk}^{int}(0) \hat{\rho}^{env}], \quad (24)$$

$$\bar{H}_{nm}^{int}(\tau) = \langle n | \hat{H}^{int}(\tau) | m \rangle, \quad (25)$$

$$\hat{H}^{int}(\tau) = e^{i\hbar\tau\hat{H}^{env}} \hat{H}^{int} e^{-i\hbar\tau\hat{H}^{env}}. \quad (26)$$

$\text{Tr}_{env}$  stands for a trace over environmental variables. The indexes  $n, m, k$ , and  $\ell$  are integers running from 0–3. The operator  $\hat{\rho}^{env}$  is the density operator for the environment. We use a secular (or rotating-wave) approximation that only retains the terms  $R_{nmk\ell}$  with  $n-m=k-\ell$ .<sup>16</sup> The Redfield relaxation tensor, Eq. (23), is related to the energy-relaxation rate  $\gamma_{nm}$  from the state  $|n\rangle$  to the state  $|m\rangle$

$$R_{nmmn} = -2 \text{Re}(\Xi_{nmmn}^{(+)}) = -\gamma_{nm} (n \neq m). \quad (27)$$

The transverse relaxation rate  $T_2^{-1}$  with respect to  $|1\rangle$  and  $|2\rangle$  is given by<sup>15</sup>

$$T_2^{-1} = \frac{1}{2} \left\{ \sum_{i=0}^3 (\gamma_{1i} + \gamma_{2i}) \right\} + \gamma_{\varphi}, \quad (28)$$

$$\gamma_{\varphi} = \text{Re}(\Xi_{1111}^{(+)} - \Xi_{1122}^{(+)} - \Xi_{2211}^{(+)} + \Xi_{2222}^{(+)}). \quad (29)$$

Equation (28) denotes the transverse relaxation rate comprising of the longitudinal relaxation term and pure dephasing term. The dissipative processes are shown in the lower part of Fig. 2. The trace term in Eq. (24) is given by

$$\begin{aligned}
& \text{Tr}_{env}[\bar{H}_{\ell m}^{int}(\tau)\bar{H}_{nk}^{int}(0)\hat{\rho}^{env}] \\
&= \chi_{\ell m}\chi_{nk}\sum_{\alpha}\lambda_{\alpha}^2\text{Tr}_{env}[e^{i\sum_{\alpha}\omega_{\alpha}(\hat{n}_{\alpha}+1/2)\tau}(\hat{a}_{\alpha}^{\dagger}+\hat{a}_{\alpha}) \\
&\quad \times e^{-i\sum_{\alpha}\omega_{\alpha}(\hat{n}_{\alpha}+1/2)\tau}(\hat{a}_{\alpha}^{\dagger}+\hat{a}_{\alpha})\hat{\rho}^{env}], \\
&= \chi_{\ell m}\chi_{nk}\sum_{\alpha}\lambda_{\alpha}^2\{e^{i\omega_{\alpha}\tau}\langle\hat{n}_{\alpha}\rangle + e^{-i\omega_{\alpha}\tau}\langle\hat{n}_{\alpha}\rangle + 1\}, \quad (30)
\end{aligned}$$

where  $\hat{n}_{\alpha}=\hat{a}_{\alpha}^{\dagger}\hat{a}_{\alpha}$ ,  $\langle\hat{n}_{\alpha}\rangle=\text{Tr}_{env}[\hat{n}_{\alpha}\hat{\rho}^{env}]=(e^{\hbar\omega_{\alpha}\beta}-1)^{-1}$ ,  $\chi_{ij}=\langle i|\hat{\chi}|j\rangle$ , and  $\beta=(k_B T)^{-1}$ . Equation (24) is then rewritten as

$$\begin{aligned}
\Xi_{\ell mnk}^{(+)} &= -\frac{i}{\hbar^2}\lim_{\epsilon\rightarrow 0}\chi_{\ell m}\chi_{nk}\sum_{\alpha}\lambda_{\alpha}^2 \\
&\quad \times \left( \frac{\langle\hat{n}_{\alpha}\rangle}{\omega_{nk}-\omega_{\alpha}-i\epsilon} + \frac{\langle\hat{n}_{\alpha}\rangle+1}{\omega_{nk}+\omega_{\alpha}-i\epsilon} \right), \quad (31)
\end{aligned}$$

where the first and second terms in brackets denote an absorption and an emission process, respectively. Using the relation  $\lim_{\epsilon\rightarrow 0}(\omega-i\epsilon)^{-1}=P[\omega^{-1}]+i\pi\delta(\omega)$  with  $P$  being a principal value, the real part of  $\Xi_{\ell mnk}^{(+)}$  is written as

$$\begin{aligned}
\text{Re}(\Xi_{\ell mnk}^{(+)}) &= \chi_{\ell m}\chi_{nk}\frac{\pi}{\hbar^2}\sum_{\alpha}\lambda_{\alpha}^2\{\langle\hat{n}_{\alpha}\rangle\delta(\omega_{nk}-\omega_{\alpha}) \\
&\quad + (\langle\hat{n}_{\alpha}\rangle+1)\delta(\omega_{nk}+\omega_{\alpha})\}, \\
&= \chi_{\ell m}\chi_{nk}J(|\omega_{nk}|)\frac{e^{-\hbar\omega_{nk}\beta/2}}{\sinh(\hbar|\omega_{nk}|\beta/2)}, \quad (32)
\end{aligned}$$

where the spectral function is given by  $J(\omega)=\pi\sum_{\alpha}\lambda_{\alpha}^2\delta(\omega_{\alpha}-\omega)/(2\hbar^2)$ .

### III. PHASE QUBIT AT OPTIMAL POINT

Let us discuss the pure dephasing rate  $\gamma_{\varphi}$ . In an Ohmic environment, the spectral density function  $J(\omega)$  is given as<sup>23</sup>  $J(\omega)=\gamma\omega f(\omega/\omega_c)=\gamma\omega\{1+(\omega/\omega_c)^2\}^{-1}$ , where  $\omega_c$  is the (Drude) cut-off frequency and  $\gamma$  is a frequency-independent coefficient. Using Eqs. (29) and (32),  $\gamma_{\varphi}$  is given by

$$\begin{aligned}
\gamma_{\varphi} &= \lim_{\omega\rightarrow 0}J(\omega)(\chi_{11}-\chi_{22})^2\frac{e^{-\hbar\omega\beta/2}}{\sinh(\hbar\omega\beta/2)}, \\
&= \lim_{\omega\rightarrow 0}\frac{\gamma\omega}{1+(\omega/\omega_c)^2}(\chi_{11}-\chi_{22})^2\frac{e^{-\hbar\omega\beta/2}}{\sinh(\hbar\omega\beta/2)}, \\
&= \lim_{\omega\rightarrow 0}\frac{\gamma\omega}{1+(\omega/\omega_c)^2}(\chi_{11}-\chi_{22})^2\frac{2}{e^{\hbar\omega\beta}-1},
\end{aligned}$$

$$\begin{aligned}
&\simeq \lim_{\omega\rightarrow 0}\gamma\omega(\chi_{11}-\chi_{22})^2\frac{2}{(1+\hbar\omega\beta)-1}, \\
&= (\chi_{11}-\chi_{22})^2\frac{2\gamma}{\hbar\beta}, \\
&= \{2(\xi_A-\xi_B)\cos\eta_{-}\}^2\frac{2\gamma}{\hbar\beta}, \quad (33)
\end{aligned}$$

where the relations  $\chi_{11}=(\xi_B-\xi_A)\cos\eta_{-}$  and  $\chi_{22}=(\xi_A-\xi_B)\cos\eta_{-}$  are used in the last equation.

Let us consider the optimal working point where the phase qubit is insensitive to the fluctuations that originate from the bias currents. Using Eq. (21) and a relation  $\partial\hat{H}^{sys}/\partial\tilde{I}_i=\partial\hat{U}/\partial\tilde{I}_i$  where the potential operator  $\hat{U}$  denotes  $\sum_{i=A,B}E_{Ji}(1-\cos\hat{\theta}_i-\tilde{I}_i\hat{\theta}_i)$ , the coefficient in Eq. (33) is rewritten as

$$\begin{aligned}
2(\xi_A-\xi_B)\cos\eta_{-} &= \sum_{i=A,B}(\langle 2|\hat{\theta}_i|2\rangle - \langle 1|\hat{\theta}_i|1\rangle), \\
&= \sum_{i=A,B}\frac{1}{E_{Ji}}\left(\langle 2|\frac{\partial\hat{H}^{sys}}{\partial\tilde{I}_i}|2\rangle - \langle 1|\frac{\partial\hat{H}^{sys}}{\partial\tilde{I}_i}|1\rangle\right), \\
&= \sum_{i=A,B}\frac{1}{E_{Ji}}\frac{\partial\hbar\omega_{21}}{\partial\tilde{I}_i}, \quad (34)
\end{aligned}$$

where we have used Hellmann-Feynman theorem<sup>26</sup> in the last equation. Here we introduce the normalized total current  $\tilde{I}_{+}=\tilde{I}_A+\tilde{I}_B$  and relative current  $\tilde{I}_{-}=\tilde{I}_A-\tilde{I}_B$  to describe a single qubit formed in the coupled CBJJs. Substituting Eq. (34) into Eq. (33), we obtain

$$\gamma_{\varphi} = \left\{ \frac{1}{2}\left(\frac{1}{E_{JA}} + \frac{1}{E_{JB}}\right)\frac{\partial\hbar\omega_{21}}{\partial\tilde{I}_{+}} + \frac{1}{2}\left(\frac{1}{E_{JA}} - \frac{1}{E_{JB}}\right)\frac{\partial\hbar\omega_{21}}{\partial\tilde{I}_{-}} \right\}^2\frac{2\gamma}{\hbar\beta}. \quad (35)$$

It turns out that pure dephasing depends on two derivatives, i.e.,  $\partial\hbar\omega_{21}/\partial\tilde{I}_{\pm}$ . The optimal point is defined as a point exhibiting a robust state against bias fluctuations and is then given by  $\partial\hbar\omega_{21}/\partial\tilde{I}_{\pm}=0$ . Here, the energy-level separation  $\hbar\omega_{21}$  between  $|1\rangle$  and  $|2\rangle$  in coupled Josephson phase qubits is expressed by

$$\hbar\omega_{21} = \sqrt{(2\varepsilon_A - 2\varepsilon_B)^2 + 4g_{-}^2}, \quad (36)$$

where the energy separation  $2\varepsilon_i$  of the  $i$ th junction is approximately given by<sup>27</sup>  $2\varepsilon_i=\hbar\omega_{pi}(1-5\hbar\omega_{pi}/36\Delta U_i)$  with  $\omega_{pi}$  being Josephson plasma frequency:

$$\omega_{pi} = \sqrt{2\pi I_c/\tilde{C}_i\Phi_0(1-\tilde{I}_i^2)^{1/4}}$$

and  $\Delta U_i$  being the depth of the potential wells:<sup>28</sup>  $\Delta U_i=2E_{Ji}\{(1-\tilde{I}_i^2)^{1/2}-\tilde{I}_i\cos^{-1}\tilde{I}_i\}$ .

Figure 3 shows the energy-level separation  $\hbar\omega_{21}$  as a function of  $\tilde{I}_{\pm}$  for nonidentical junctions. The junction parameters are given by<sup>29</sup>  $I_{cA(B)}=I_0[1+(-)a_I]$  and  $C_{A(B)}$

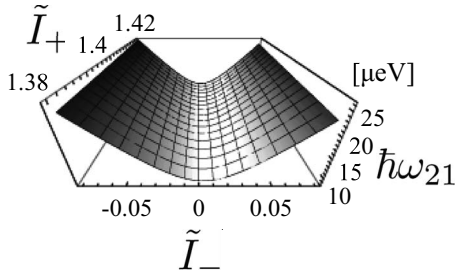


FIG. 3. Energy-level separation  $\hbar\omega_{21}$  as a function of  $\tilde{I}_{\pm}$  for nonidentical junctions the parameters  $I_0=1 \mu\text{A}$ ,  $a_I=0.02$ ,  $C_0=10 \text{ fF}$ , and  $a_c=0.02$ . Here the number of levels is restricted to two within the range  $0.66 \leq \tilde{I}_{A,B} \leq 0.74$ .

$=C_0[1+(-)a_c]$ , where  $I_0$  and  $C_0$  are the averages of the critical currents and the capacitances, respectively; the asymmetric parameters  $a_I$  and  $a_c$  are then defined as  $(I_{cA}-I_{cB})/2I_0$  and  $(C_A-C_B)/2C_0$ , respectively. The energy-level separation shows almost no dependence on the total current flowing through the entire system  $\tilde{I}_{+}$ . This means that the coupled qubit is inherently stable against  $\tilde{I}_{+}$ . In addition, the energy-level separation  $\hbar\omega_{21}$  changes *nonmonotonically* along the  $\tilde{I}_{-}$  coordinate and has an extreme value. This implies  $\partial\hbar\omega_{21}/\partial\tilde{I}_{-}=0$ , leading to an optimal point. On the other hand, the energy separation  $2\varepsilon_i$  of a conventional phase qubit changes monotonically with a bias current. Therefore, the conventional phase qubit has no optimal point since  $\partial\varepsilon_i/\partial\tilde{I}_i \neq 0$  for any bias. Figure 4 shows the pure dephasing rate  $\gamma_{\phi}$  as a function of  $\tilde{I}_{\pm}$ . It turns out that there are two zero lines on the pure dephasing rate  $\gamma_{\phi}$ . One line ( $L_1$ ) located near  $\tilde{I}_{-}=0.003$  gives the optimal operation points while the other ( $L_2$ ) does not, even with zero pure dephasing. Figure 5 shows  $\partial\hbar\omega_{21}/\partial\tilde{I}_{\pm}$  as functions of  $\tilde{I}_{-}$  and explains the difference between lines  $L_1$  and  $L_2$ . The derivatives  $\partial\hbar\omega_{21}/\partial\tilde{I}_{\pm}$  for the  $L_1$  line *simultaneously* become zero at the bias point that satis-

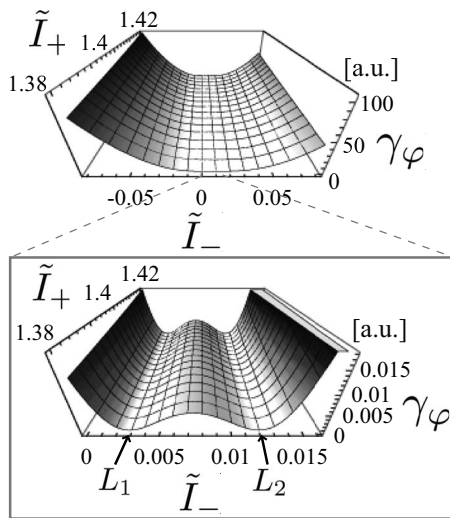


FIG. 4. The pure dephasing rate  $\gamma_{\phi}$  as a function of  $\tilde{I}_{\pm}$  for the nonidentical junctions with parameters  $I_0=1 \mu\text{A}$ ,  $a_I=0.02$ ,  $C_0=10 \text{ fF}$ , and  $a_c=0.02$ .

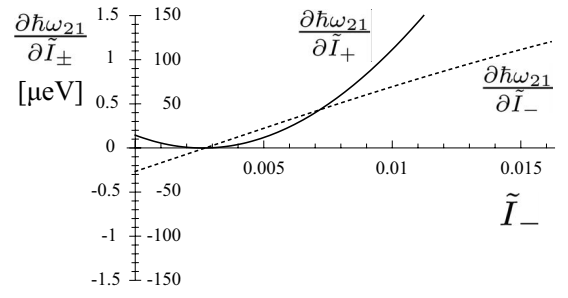


FIG. 5. Derivatives of  $\hbar\omega_{21}$  with respect to  $\tilde{I}_{\pm}$  as functions of  $\tilde{I}_{-}$  ( $\tilde{I}_{+}=1.4$ ). The solid and dashed lines denote the differentiations  $\partial\hbar\omega_{21}/\partial\tilde{I}_{+}$  (left label of vertical axis) and  $\partial\hbar\omega_{21}/\partial\tilde{I}_{-}$  (right label of vertical axis), respectively. Both lines meet at zero points where it is on the minimal line  $L_1$  in Fig. 4.

fies  $\varepsilon_A=\varepsilon_B$  since the derivatives  $\partial\hbar\omega_{21}/\partial\tilde{I}_{\pm}$  share the same factor  $\varepsilon_A-\varepsilon_B$

$$\frac{\partial\hbar\omega_{21}}{\partial\tilde{I}_{\pm}} = \frac{2(\varepsilon_A - \varepsilon_B)}{\sqrt{(\varepsilon_A - \varepsilon_B)^2 + g^2}} \frac{\partial(\varepsilon_A - \varepsilon_B)}{\partial\tilde{I}_{\pm}}. \quad (37)$$

This is simply the definition of the optimal operation point since the derivatives  $\partial\hbar\omega_{21}/\partial\tilde{I}_{\pm}$  measure the tolerance for fluctuations. In contrast, the  $L_2$  line emerges from the balance between the two terms in curly brackets in Eq. (35).

With the identical junctions ( $a_I=a_c=0$ ), the minimal line is formed at  $\tilde{I}_{-}=0$ . While, with the asymmetric junctions, the minimal line is formed at  $\tilde{I}_{-} \neq 0$  because the asymmetric parameters  $a_I$  and  $a_c$  modify the energy separations  $2\varepsilon_{A,B}$ . Figure 6 shows the optimal points as functions of the asymmetric parameters  $a_I$  and  $a_c$ . There are optimal points in all accessible parameter ranges where the number of levels is restricted to two.

#### IV. CONCLUSION

The pure dephasing that destroys coherence without a change in the two-level populations is one of the decoherence mechanisms in a qubit caused by low-frequency fluc-

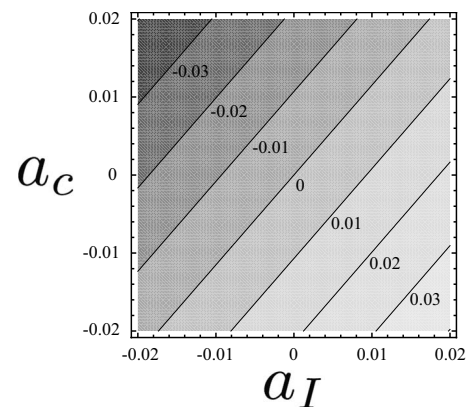


FIG. 6. Current  $\tilde{I}_{-}$  at an optimal point as functions of asymmetric parameters  $a_I$  and  $a_c$  ( $\tilde{I}_{+}=1.4$ ).

tuations. This can be greatly suppressed at an optimal operation point where the qubit is insensitive to bias fluctuations. However, unlike flux and charge qubits, there are no optimal points in a conventional *phase* qubit since the qubit energy splitting becomes monotonically smaller with increasing the bias current. Here we propose a phase qubit with an optimal point by introducing the qubit energy splitting nonmonotonically depending on the current bias realized in capacitively coupled Josephson junctions. We have studied pure dephasing in coupled Josephson-phase qubits within the Bloch-Redfield formalism, in order to obtain an analytic expression for the pure dephasing rate. We have demonstrated that capacitively coupled phase qubits act as a single phase qubit with an optimal point. In addition, we found that there are optimal points at all accessible asymmetric junctions.

### ACKNOWLEDGMENTS

We are grateful to Munehiro Nishida for valuable discussions. This work was supported in part by KAKENHI (Nos. 195485, 195836, and 18540352) from MEXT of Japan.

### APPENDIX

In this appendix, we derive the system Hamiltonian consisting of the coupled Josephson junction system interacting with the environment from the following Lagrangian  $\mathcal{L}^{sys}$  given as:<sup>30</sup>

$$\mathcal{L}^{sys} = \sum_{i=A,B} (K_i - U_i) + K_c, \quad (\text{A1})$$

$$K_i = \frac{1}{2} C_i V_i^2 = \frac{1}{2} C_i \left( \frac{\Phi_0}{2\pi} \right)^2 \dot{\theta}_i^2, \quad (\text{A2})$$

$$U_i = E_J (1 - \cos \theta_i - \tilde{I}_i \theta_i), \quad (\text{A3})$$

$$K_c = \frac{1}{2} C_c (V_A - V_B)^2 = \frac{1}{2} C_c \left( \frac{\Phi_0}{2\pi} \right)^2 (\dot{\theta}_A - \dot{\theta}_B)^2. \quad (\text{A4})$$

Here  $K_i$  and  $U_i$  denote the charging energy and the Josephson potential energy of the  $i$ th junction, respectively.  $V_i$  is the voltage across the  $i$ th junction.  $K_c$  is the charging energy of a coupling capacitor. The total charging energy  $\sum_{i=A,B} K_i + K_c$  is written as

$$\sum_{i=A,B} K_i + K_c = \frac{1}{2} \left( \frac{\Phi_0}{2\pi} \right)^2 \dot{\theta}^T \hat{C} \dot{\theta} \quad (\text{A5})$$

with

$$\hat{C} = \begin{pmatrix} C_A + C_c & -C_c \\ -C_c & C_B + C_c \end{pmatrix}, \quad (\text{A6})$$

where the vector  $\theta$  is given by  $(\theta_A, \theta_B)^T$  with  $T$  being the transpose. Using the vector  $\mathbf{p} = (\Phi_0/2\pi) \hat{C} \dot{\theta} = (p_A, p_B)^T$  where  $p_i$  corresponds to the canonical momentum  $(2\pi/\Phi_0) \partial \mathcal{L}^{sys} / \partial \dot{\theta}_i$ , Eq. (A5) is transformed into

$$\frac{1}{2} \left( \frac{\Phi_0}{2\pi} \dot{\theta}^T \right) \frac{\Phi_0}{2\pi} \hat{C} \dot{\theta} = \frac{1}{2} (\mathbf{p}^T \hat{C}^{-1}) \mathbf{p}. \quad (\text{A7})$$

Then, the system Hamiltonian  $H^{sys}$  is written as

$$\begin{aligned} H^{sys} &= \frac{\Phi_0}{2\pi} \sum_{i=A,B} p_i \dot{\theta}_i - \mathcal{L}^{sys}, \\ &= \sum_{i=A,B} p_i \left( \frac{\Phi_0}{2\pi} \dot{\theta}_i \right) - \frac{1}{2} \mathbf{p}^T \hat{C}^{-1} \mathbf{p} + \sum_{i=A,B} U_i, \\ &= \mathbf{p}^T (\hat{C}^{-1} \mathbf{p}) - \frac{1}{2} \mathbf{p}^T \hat{C}^{-1} \mathbf{p} + \sum_{i=A,B} U_i, \\ &= \frac{1}{2} \mathbf{p}^T \hat{C}^{-1} \mathbf{p} + \sum_{i=A,B} U_i, \end{aligned} \quad (\text{A8})$$

where the matrix  $\hat{C}^{-1}$  is given by

$$\begin{aligned} \hat{C}^{-1} &= \frac{1}{\det \hat{C}} \begin{pmatrix} C_B + C_c & C_c \\ C_c & C_A + C_c \end{pmatrix}, \\ &= \begin{pmatrix} \tilde{C}_{AA}^{-1} & \tilde{C}_{AB}^{-1} \\ \tilde{C}_{BA}^{-1} & \tilde{C}_{BB}^{-1} \end{pmatrix}. \end{aligned} \quad (\text{A9})$$

Here the determinant of the  $\hat{C}$  matrix,  $\det \hat{C}$ , is given by  $C_A(C_B + C_c) + C_B C_c = C_B(C_A + C_c) + C_A C_c$ . The matrix element  $\tilde{C}_{ii}$  in the diagonal elements of the matrix, Eq. (A9), is given by

$$\begin{aligned} \tilde{C}_{ii} &= \frac{\det \hat{C}}{C_j + C_c}, \quad i \neq j, \\ &= \frac{C_i(C_j + C_c) + C_j C_c}{C_j + C_c}, \\ &= C_i + (C_j^{-1} + C_c^{-1})^{-1} = \tilde{C}_i. \end{aligned} \quad (\text{A10})$$

The matrix element  $\tilde{C}_{ij}$  in the off-diagonal elements of the matrix, Eq. (A9), is written as

$$\begin{aligned} \tilde{C}_{ij} &= \frac{\det \hat{C}}{C_c}, \\ &= \frac{\det \hat{C} / \sqrt{(C_A + C_c)(C_B + C_c)}}{C_c / \sqrt{(C_A + C_c)(C_B + C_c)}}, \\ &= \frac{\sqrt{\det \hat{C} / (C_B + C_c)} \sqrt{\det \hat{C} / (C_A + C_c)}}{\sqrt{C_c / (C_A + C_c)} \sqrt{C_c / (C_B + C_c)}}, \\ &= \sqrt{\frac{\tilde{C}_A \tilde{C}_B}{\delta_A \delta_B}} = \tilde{C}_{ji}, \end{aligned} \quad (\text{A11})$$

where  $\delta_i$  is given by  $C_c/(C_i+C_c)$ . Using Eqs. (A10) and (A11), the system Hamiltonian is rewritten as<sup>18,19</sup>

$$H^{\text{sys}} = \frac{1}{2} \sum_{i=A,B} \sum_{j=A,B} p_i \tilde{C}_{ij}^{-1} p_j + \sum_{i=A,B} U_i,$$

$$= \sum_{i=A,B} \left( \frac{p_i^2}{2\tilde{C}_{ii}} + U_i \right) + \left( \frac{p_A p_B}{2\tilde{C}_{AB}} + \frac{p_A p_B}{2\tilde{C}_{BA}} \right),$$

$$= \sum_{i=A,B} \left( \frac{p_i^2}{2\tilde{C}_i} + U_i \right) + \sqrt{\delta_A \delta_B} \frac{p_A p_B}{\sqrt{\tilde{C}_A \tilde{C}_B}}. \quad (\text{A12})$$

- 
- <sup>1</sup>J. E. Mooij, T. P. Orlando, L. Levitov, L. Tian, C. H. van der Wal, and S. Lloyd, *Science* **285**, 1036 (1999).
- <sup>2</sup>I. Chiorescu, Y. Nakamura, C. J. P. M. Harmans, and J. E. Mooij, *Science* **299**, 1869 (2003).
- <sup>3</sup>Y. Nakamura, C. D. Chen, and J. S. Tsai, *Phys. Rev. Lett.* **79**, 2328 (1997).
- <sup>4</sup>Y. Nakamura, Y. A. Pashkin, and J. S. Tsai, *Nature (London)* **398**, 786 (1999).
- <sup>5</sup>R. C. Ramos, M. A. Gubrud, A. J. Berkley, J. R. Anderson, C. J. Lobb, and F. C. Wellstood, *IEEE Trans. Appl. Supercond.* **11**, 998 (2001).
- <sup>6</sup>S. Han, Y. Yu, X. Chu, S. I. Chu, and Z. Wang, *Science* **293**, 1457 (2001).
- <sup>7</sup>J. M. Martinis, S. Nam, J. Aumentado, and C. Urbina, *Phys. Rev. Lett.* **89**, 117901 (2002).
- <sup>8</sup>Y. Makhlin, G. Schön, and A. Shnirman, in *Exploring the Quantum-Classical Frontier*, edited by J. R. Friedman and S. Han (Nova Science, Commack, NY, 2002), pp. 405–440.
- <sup>9</sup>Y. Zhang, H. N. Yeung, M. O'Donnell, and P. L. Carson, *J. Magn. Reson. Imaging* **8**, 675 (1998).
- <sup>10</sup>J. Schrieffer, Y. Makhlin, A. Shnirman, and G. Schön, *New J. Phys.* **8**, 1 (2006).
- <sup>11</sup>A. A. Houck, J. A. Schreier, B. R. Johnson, J. M. Chow, J. Koch, J. M. Gambetta, D. I. Schuster, L. Frunzio, M. H. Devoret, S. M. Girvin, and R. J. Schoelkopf, *Phys. Rev. Lett.* **101**, 080502 (2008).
- <sup>12</sup>P. Bertet, I. Chiorescu, G. Burkard, K. Semba, C. J. P. M. Harmans, D. P. DiVincenzo, and J. E. Mooij, *Phys. Rev. Lett.* **95**, 257002 (2005).
- <sup>13</sup>D. Vion, A. Aassime, A. Cottet, P. Joyez, H. Pothier, C. Urbina, D. Esteve, and M. H. Devoret, *Science* **296**, 886 (2002).
- <sup>14</sup>E. Hoskinson, F. Lecocq, N. Didier, A. Fay, F. W. J. Hekking, W. Guichard, O. Buisson, R. Dolata, B. Mackrodt, and A. B. Zorin, *Phys. Rev. Lett.* **102**, 097004 (2009).
- <sup>15</sup>F. Bloch, *Phys. Rev.* **105**, 1206 (1957).
- <sup>16</sup>A. G. Redfield, *IBM J. Res. Dev.* **1**, 19 (1957).
- <sup>17</sup>U. Weiss, *Quantum Dissipative Systems*, 3rd ed. (World Scientific, Singapore, 2008).
- <sup>18</sup>P. R. Johnson, F. W. Strauch, A. J. Dragt, R. C. Ramos, C. J. Lobb, J. R. Anderson, and F. C. Wellstood, *Phys. Rev. B* **67**, 020509(R) (2003).
- <sup>19</sup>A. Blais, A. Maassen van den Brink, and A. M. Zagoskin, *Phys. Rev. Lett.* **90**, 127901 (2003).
- <sup>20</sup>G. H. Wannier, *Phys. Rev.* **117**, 432 (1960).
- <sup>21</sup>M. Glück, A. Kolovsky, and H. J. Korsch, *J. Phys. A* **32**, L49 (1999).
- <sup>22</sup>M. Scala, R. Migliore, and A. Messina, *J. Phys. A: Math. Theor.* **41**, 435304 (2008).
- <sup>23</sup>A. O. Caldeira and A. J. Leggett, *Ann. Phys.* **149**, 374 (1983).
- <sup>24</sup>A. I. Larkin and Yu. N. Ovchinnikov, *Zh. Eksp. Teor. Fiz.* **91**, 318 (1986) [*Sov. Phys. JETP* **64**, 185 (1986)].
- <sup>25</sup>K. S. Chow, D. A. Browne, and V. Ambegaokar, *Phys. Rev. B* **37**, 1624 (1988).
- <sup>26</sup>R. P. Feynman, *Phys. Rev.* **56**, 340 (1939).
- <sup>27</sup>J. M. Martinis, S. Nam, J. Aumentado, K. M. Lang, and C. Urbina, *Phys. Rev. B* **67**, 094510 (2003).
- <sup>28</sup>T. A. Fulton and L. N. Dunkleberger, *Phys. Rev. B* **9**, 4760 (1974).
- <sup>29</sup>Y. C. Chen, *J. Low Temp. Phys.* **65**, 133 (1986).
- <sup>30</sup>A. Galiutdinov, *Phys. Rev. B* **73**, 064509 (2006).